An apparent inductance online identification for sensorless control of permanent magnet synchronous motor

Ge Yang,[1,✉] Song Weizhang,[1] Patrick Wheeler,[2] and Yang Yang[1]

[1] *Department of Power Electronics and Motor, Xi'an University of Technology, Xi'an, China*

[2] *Department of Electrical and Electronic Engineering, University of Nottingham, Nottingham, UK*

✉ E-mail: gy@xaut.edu.cn

The model-based sensorless control of permanent magnet synchronous motor (PMSM) relies on the motor parameters. In practice, the considerable uncertainty of inductance and the difference between the apparent inductance and the incremental inductance exists. To overcome it, an online apparent inductance identification method for PMSM sensorless control is proposed. First, an initial incremental inductance table (IIT) is obtained offline. Then, an asymmetric high-frequency square wave injection method is proposed to identify the incremental inductance at the operation point, and an adaptive minimum adjustment algorithm is proposed to adjust IIT automatically. Finally, the apparent inductance is calculated using the adjusted IIT. Based on it, the complete PMSM sensorless control is designed. The experimental results indicate this method is feasible and effective.

Introduction: The sensorless control of permanent magnet synchronous motor (PMSM) can improve the system reliability, reduce the cost and be benefit for high-speed operation. The model-based sensorless control method, in which the accurate motor parameters are required, is most widely used at medium-high speed region [1, 2]. But the inductance value will be effected by the magnetic saturation, high-frequency harmonics, high temperature, and varying working condition. So the online inductance identification is necessary for high-performance PMSM sensorless control.

Currently, some identification methods have been investigated [3–5]. Among them, the high-frequency voltage injection is a kind of effective method. By injecting the high-frequency voltage, the extra equation can be established, which provides the information for inductance estimation [5]. However, since the larger amplitude of injected voltage is required to obtain the enough signal-to-noise ratio of current, the DC voltage utilization rate will be greatly reduced. So this method is hard to be applied at high speed region. Furthermore, only the incremental inductance can be obtained by the signal injection type method, but the apparent inductance is required in sensorless control.

The offline identification of the inductance table under different currents is also a commonly used method. This method can effectively reduce the inductance error caused by current changing. But, since the offline identification is carried out at standstill [6], and the apparent inductance will decrease with the increasing of high-frequency harmonics and the temperature [7, 8], this varying cannot be taken into account in offline identification.

This letter presents an online apparent inductance identification method for PMSM sensorless control. In this method, the initial inductance table is constructed offline and adjusted online based on asymmetric high-frequency square wave (AHFS) injection and adaptive minimum adjustment (AMA) algorithm. This method overcomes the difficulties of online identification of apparent inductance under sensorless control.

Principle of proposed identification method: The active flux of PMSM is

$$\begin{cases} \psi_{r\alpha} = \int_0^t (u_\alpha - R_s i_\alpha)\mathrm{d}t - L_{qa} i_a \\ \psi_{r\beta} = \int_0^t (u_\beta - R_s i_\beta)\mathrm{d}t - L_{qa} i_\beta \end{cases} \tag{1}$$

where R_s is the rotor resistance, L_{qa} denotes the q-axis apparent inductance, u_α, u_β, i_α, i_β, $\psi_{r\alpha}$, and $\psi_{r\beta}$ denote the $\alpha\beta$-axis voltages, currents and active fluxes. Since $\psi_{r\alpha}$ and $\psi_{r\beta}$ contain the rotor position information, it is necessary to estimate them for sensorless control. From Equation (1), we can see L_{qa} is required in flux estimation.

Table 1. Initial incremental inductance table (IIT)

i_d \ i_q	0 A	1 A	2 A	3 A	4 A	5 A
0 A	0.029	0.026	0.024	0.021	0.021	0.020
1 A	0.028	0.025	0.023	0.022	0.021	0.020
2 A	0.027	0.023	0.022	0.021	0.020	0.019
3 A	0.025	0.023	0.021	0.020	0.019	0.019
4 A	0.024	0.022	0.021	0.020	0.018	0.018
5 A	0.024	0.022	0.019	0.019	0.018	0.017

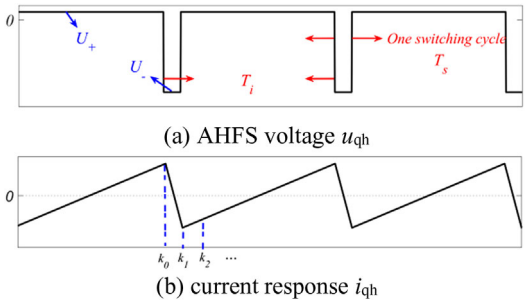

Fig. 1 *Diagram of AHFS voltage and current response*

First, the initial incremental inductance table (IIT) need to obtain offline. To this end, the rotor is locked and the motor operates at current control mode. Then, the high-frequency q-axis square wave voltage is injected under different i_d and i_q. The incremental inductance can be calculated using the high-frequency voltage equation, i.e. $u_{qh} = L_{qi}\mathrm{d}i_q/\mathrm{d}t$, where L_{qi} denote incremental inductance. For the PMSM in experiment, the initial IIT is obtained as Table 1. Since the second-order difference of IIT is smaller and IIT will be adjusted in real time, the step size of the table is allowed to be selected larger to save storage space.

Next, the incremental inductance at the operation point is estimated in real time using the AHFS injection method. Figure 1 presents the diagram of the AHFS voltage and the current response. When motor rotates forward, the AHFS voltage consists of a larger negative voltage which lasts fewer switching cycles and a smaller positive voltage which lasts more switching cycles. Since the positive voltage is smaller, the problem that the DC voltage is not enough for signal injection at high-speed region can be solved, which will expand the speed range of the identification method.

If the negative voltage lasts one switching cycle, the current response can be express as

$$\begin{cases} i_{qh}(k_0) = -i_{qh}(k_1) \\ i_{qh}(k_2) - i_{qh}(k_1) = -\frac{i_{qh}(k_1) - i_{qh}(k_0)}{n-1} \\ i_{qh}(k_3) - i_{qh}(k_2) = -\frac{i_{qh}(k_1) - i_{qh}(k_0)}{n-1} \\ \vdots \\ i_{qh}(k_n) - i_{qh}(k_{n-1}) = -\frac{i_{qh}(k_1) - i_{qh}(k_0)}{n-1} \end{cases} \tag{2}$$

where subscript "h" denote the high-frequency component of current, $n = T_i/T_s$ denotes the ratio of injected voltage cycle to switching cycle, and k_0, k_1, k_2, …, denote the discrete time points. Let m denote the ratio of U_+ action time to switching cycle, there is $|U_+/U_-| = (n-m)/m$. If necessary, we can reduce m to avoid $|R_s i_q + \omega L_d i_d + \omega\psi_f + U_-| \geq \sqrt{U_s^2 - u_d^2}$ at lower speed.

Assuming in one switching cycle, the fundamental wave of current is constant, i.e. $i_{qF}(k_0) = i_{qF}(k_1)$, where subscript "F" denote the fundamental wave, we can get

$$\begin{cases} i_{qF}(k_0) = i_{qF}(k_1) = \frac{i_q(k_0) + i_q(k_1)}{2} \\ i_{qj}(k_0) = -i_{qj}(k_1) = \frac{i_q(k_0) - i_q(k_1)}{2} \end{cases} \tag{3}$$

Using Equation (3) and voltage equation of PMSM, we have

$$L_{qi}\frac{i_q(k_1)-i_q(k_0)}{\Delta t}=u_{qj} \tag{4}$$

where L_{qi} denote the incremental inductance. Then, L_{qi} can be estimated as

$$\frac{\mathrm{d}\hat{L}_{\mathrm{qi}}}{\mathrm{d}t}=\lambda i_{qj}(k_1)[u_{qj}\Delta t-\hat{L}_{qi}(i_q(k_1)-i_q(k_0))] \tag{5}$$

where λ determines the convergence rate. The incremental inductance at one certain operation point can be estimated by this method. The convergence of Equation (5) can be proved by defining a function as $V=0.5[u_{qj}\Delta t-\hat{L}_{qi}(i_q(k_1)-i_q(k_0))]^2$ and deducing its derivative.

The design criteria of AHFS is introduced here. First, according to the rated speed, rated torque and U_{dc}, we can calculate U_+. Next, calculate the action time of U_+ according to the required amplitude of current response. Then, determine U_- according to the equation $m_{\max}=|U_-/U_+|=n-1$. At lower speed, m can be adjusted smaller to reduce $|U_-|$ if necessary.

Assuming the estimated incremental inductance is $\hat{L}_{qi}(i_{dw}, i_{qw})$ where i_{dw} and i_{qw} denote the current of the operation point, then the data in IIT need to be adjusted accordingly. Let $L_{qi}(i_d,i_q)$and $\hat{L}_{qi}(i_d, i_q)$ denote the incremental inductance in IIT before and after adjustment. The adjustment algorithm is presented here.

It is reasonable to assume the accurate IIT should be around the initial IIT and satisfy the estimated incremental inductance at working point. Therefore, if i_d,$i_q = i_{dw}$,i_{qw}, $L_{\mathrm{qi}}(i_{\mathrm{d}},i_{\mathrm{q}})$ will be adjusted as $\hat{L}_{\mathrm{qi}}(i_{\mathrm{d}}, i_{\mathrm{q}}) = \hat{L}_{\mathrm{qi}}(i_{\mathrm{dw}}, i_{qw})$, i.e. equal to the online estimation value at working point. If i_d,$i_q \neq i_{dw}$,i_{qw}, $\hat{L}_{qi}(i_d, i_q)$ will be obtained in the case that the following function is minimum

$$S_{ad}=\left(\frac{\hat{L}_{qi}(i_d,i_q)-L_{qi}(i_d,i_q)}{L_{qi}(i_d,i_q)}\right)^2+\left(\frac{[\hat{L}_{qi}(i_d,i_q)-\hat{L}_{qi}(i_{dw},i_{qw})]-[L_{qi}(i_d,i_q)-L_{qi}(i_{dw},i_{qw})]}{L_{qi}(i_d,i_q)-L_{qi}(i_{dw},i_{qw})}\right)^2 \tag{6}$$

We can see that S_{ad} is sum of relative variation from $\hat{L}_{qi}(i_d, i_q)$ to $L_{qi}(i_d,i_q)$ and $\hat{L}_{qi}(i_d, i_q)-\hat{L}_{qi}(i_{dw}, i_{qw})$ to $L_{qi}(i_d,i_q)-L_{qi}(i_{dw},i_{qw})$. So, S_{ad} can be viewed as the IIT variation after adjusted, which includes the variation of every data and their relationship.

When S_{ad} is minimum, we have

$$\frac{\partial S_{ad}}{\partial \hat{L}_{qi}(i_d,i_q)}=0 \tag{7}$$

Substituting Equation (6) into Equation (7), it yields

$$\hat{L}_{qi}(i_d,i_q)=\frac{AB+AC}{A+B} \tag{8}$$

where $A = L_{qi}(i_d,i_q)$, $B = L_{qi}(i_d,i_q) - L_{qi}(i_{dw},i_{qw})$ and $C = \hat{L}_{qi}(i_{dw}, i_{qw}) + L_{qi}(i_d, i_q) - L_{qi}(i_{dw}, i_{qw})$. Since S_{ad} describes the adjustment degree of IIT, this algorithm is called as AMA. Using Equation (8), every data in IIT will be updated. Then, the apparent inductance can be calculated as

$$L_{qa}(i_{dw})=\frac{\int_0^{i_{qw}}\hat{L}_{qi}(i_{dw},i_q)\mathrm{d}i_q}{i_{qw}} \tag{9}$$

Due to the limited calculation ability of processor, above calculation cannot be finished in one switching cycle. So, in each cycle, only one data in IIT is adjusted, and one accumulation of Equation (9) is carried out. If IIT contains k^2 data, above adjustment process requires k^2 cycles, and the apparent inductance calculation requires k cycles, which will not influence the real-time property. In addition, the apparent inductance is also updated in sensorless control in real time. Since the incremental inductance at operation point is estimated gradually, the identified apparent inductance changes slightly in one updating. So the stability can be ensured.

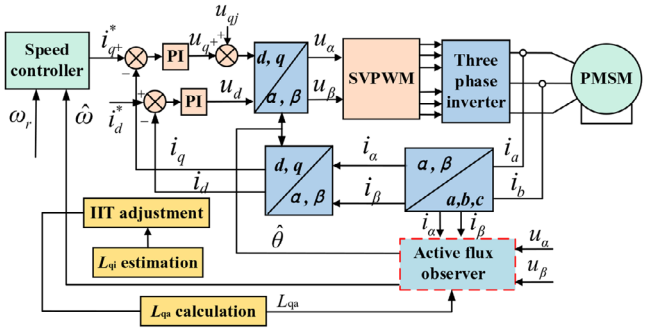

Fig. 2 *Diagram of AHFS voltage and current response*

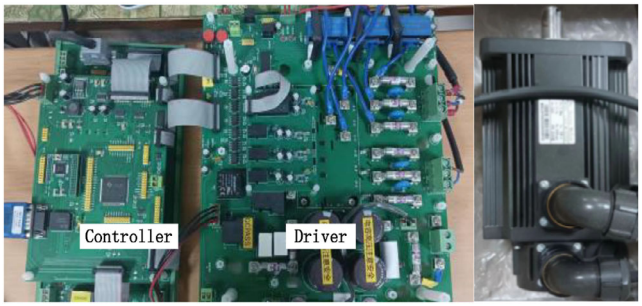

Fig. 3 *Experimental platform*

Table 2. Incremental inductance table after adjustment

i_d \ i_q	0 A	1 A	2 A	3 A	4 A	5 A
0 A	0.0279	0.0249	0.0229	0.0197	0.0197	0.0190
1 A	0.0269	0.0238	0.0219	0.0207	0.0197	0.0186
2 A	0.0258	0.0225	0.0207	0.0197	0.0186	0.0186
3 A	0.0236	0.0218	0.0195	0.0186	0.0176	0.0165
4 A	0.0227	0.0197	0.0186	0.0186	0.0165	0.0165
5 A	0.0218	0.0197	0.0175	0.0172	0.0165	0.0154

Then, the complete sensorless control of PMSM is designed as shown in Figure 2. The flux is estimated by the active flux observer [2], and the position and speed are estimated simultaneously. The q-axis apparent inductance is identified online by the proposed method, and feedback to the flux observer. The estimated position and speed are used for coordinate transformation and speed control.

Experiment results: In this section, the experiments are carried out. The experimental platform is shown in Figure 3. The control algorithm is realized by the processor TMS320F28335. A three phase IGBT inverter, supplied by the DC voltage of 450 V, feeds the PMSM, whose rotor flux is 0.075 Wb and d-axis inductance is 108 mH. An incremental encoder of 2500 lines is used to detect the real position and speed. The switching frequency of the inverter is 10 kHz, the frequencies of the current and speed controller are 10 and 5 kHz, and the dead time is set as 2.4 μs. Considering the incremental inductance table is used in which the inductance varying with the current has been taken into account, λ can be chosen smaller to ensure the stability. Here, λ is chosen as 0.02.

Figures 4 and 5 present the results under 1.8 times overload condition, where $i_d = 3$ A and $i_q = 5$ A. Figure 4(a) shows the identification results of incremental inductance, where the initial value of L_{qa} and L_{qi} are set as 29 and 22 mH. We can see the estimated L_{qi} converges to 16.5 mH with the AHFS injection method. Figure 4(b) and Table 2 show the curve surface of L_{qi} and IIT after adjustment by AMA algorithm. Then, the apparent inductance at operation point is calculated as 19.6 mH.

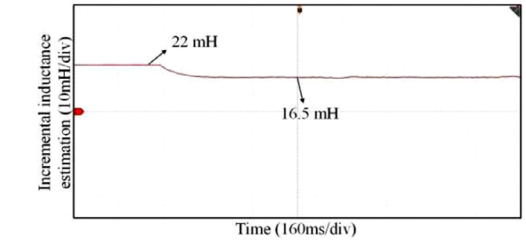

(a) The q-axis incremental inductance identification result

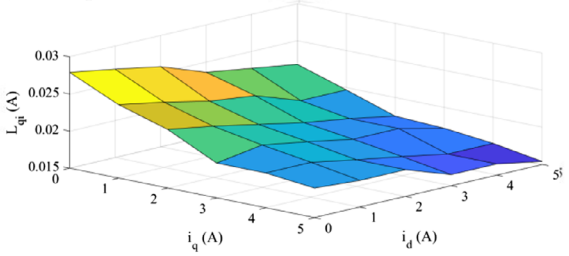

(b) The curve surface of L_{qi} after adjustment

Fig. 4 *The incremental inductance identification results*

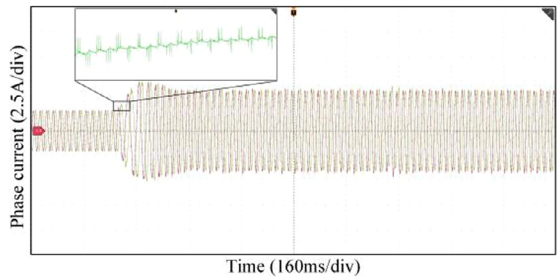

(a) Phase current

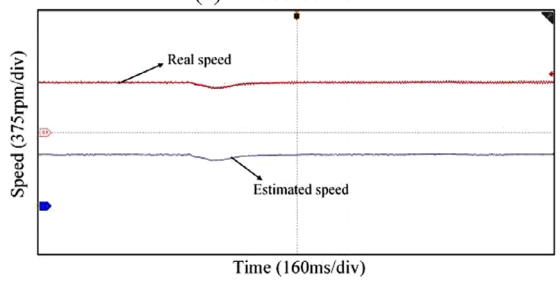

(b) Speed estimation

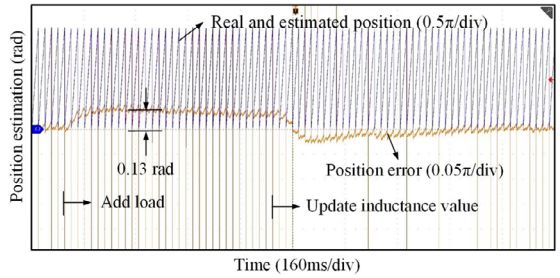

(c) Position estimation

Fig. 5 *The results under 1.8 times overload*

Figure 5 shows the current, speed and position estimation results under 1.8 times overload condition, and the starting state is no-load. The initial value of L_{qa} is set as 29 mH, and it is updated after adding load. We can see when the load is added, since the inductance error exists, the position error is about 0.13 rad, which agrees well with the theoretical calculation. Then, the position error converges to about zero after the updating of apparent inductance, which proves the accuracy of the inductance identification.

Conclusions: This letter proposes an apparent inductance online identification method for PMSM sensorless control. Using the AHFS injection, the incremental inductance at the operation point is estimated, and using the AMA algorithm, the IIT is adjusted online. Then, the apparent inductance is calculated with IIT after adjustment. The experiment results indicate that this method is feasible and effective on improving the sensorless control performance.

Author contributions: **Ge Yang**: Conceptualization; methodology; formal analysis; writing—original draft. **Song Weizhang**: Project administration; data curation; supervision. **Patrick Wheeler**: Funding acquisition; writing—review & editing. **Yang Yang**: Validation.

Conflict of interest statement: The authors declare no conflicts of interest.

Funding information: Ministry of Science and Technology of the People's Republic of China National Natural Science Foundation of China 51877176. Shaanxi Provincial Science and Technology Department Natural Science Basic Research Program of Shaanxi Province 2024JC-YBQN-0546. China Postdoctoral Science Foundation Postdoctoral Research Foundation of China 2023MD744252. Shaanxi Province Postdoctoral Research Project Funding 2023BSHYD22139.

Data availability statement: All relevant data are within the paper.

Received: *8 January 2024* Accepted: *12 May 2024*
doi: 10.1049/ell2.13233

References

1 Park, S., Woo, T., Choi, S., et al.: Mitigating rotor movement during estimation of flux saturation model at standstill for IPMSMs and SynRMs. *IEEE Trans. Ind. Electron.* **70**(2), 1171–1181 (2023)
2 Ge, Y., Song, W.Z., Yang, Y., et al.: A polar-coordinate-multisignal-flux-observer-based PMSM non-PLL sensorless control. *IEEE Trans. Power Electron.* **38**(9), 10578–10583 (2023)
3 Bui, M.X., Rahman, M.F., Guan, D.Q.: A new and fast method for online estimation of d and q axes inductance of interior permanent magnet synchronous machines using measurements of current derivatives and inverter DC-bus voltage. *IEEE Trans. Power Electron.* **66**(10), 7488–7497 (2019)
4 Liu, S., Wang, Q., Wang, G., et al.: Virtual-axis injection based online para- meter identification of PMSM considering cross coupling and saturation effects. *IEEE Trans. Power Electron.* **38**(5), 5791–5802 (2023)
5 Omer, C.K., Salih, B.O.: Sensorless PMSM drive based on stator feed forward voltage estimation improved with MRAS multiparameter estimation. *IEEE-ASME Trans. Mechatron.* **23**(3), 1326–1337 (2018)
6 Marko, H., Paolo, P., Eemeli, M., et al.: Sensorless self-commissioning of synchronous reluctance motors at standstill without rotor locking. *IEEE Trans. Ind. Appli.* **53**(3), 2120–2129 (2017)
7 Zhu, S., Hua, W., Shi, B.: Comparison of methods using different sources for computing PWM effects on permanent magnet machines considering eddy current reaction. *IEEE Trans. Magn.* **57**(7), 1–4 (2021). https://doi.org/10.1109/TMAG.2021.3066418
8 Chen, D.Z., Zhang, Y.Y., Bai, B.D., et al.: Electromagnetic-force and vibration of silicon steel sheet and variable frequency motor under different temperature and harmonic. *CES Trans. Electr. Mach. Syst.* **35**(22), 4647–4656 (2020)